

ARTICLE

Expression, Localization, and Binding Activity of the Ezrin/Radixin/Moesin Proteins in the Mouse Testis

Tomohiko Wakayama, Hiroki Nakata, Miho Kurobo, Yoshimichi Sai, and Shoichi Iseki

Department of Histology and Embryology, Graduate School of Medical Science, Kanazawa University, Kanazawa, Japan (TW,HN,MK,SI), and Department of Pharmaceutics, Faculty of Pharmacy, Keio University, Tokyo, Japan (YS)

SUMMARY The ezrin, radixin, and moesin (ERM) proteins represent a family of adaptor proteins linking transmembrane proteins to the cytoskeleton. The seminiferous epithelium undergoes extensive changes in cellular composition, location, and shape, implicating roles of the membrane–cytoskeleton interaction. It remains unknown, however, whether the ERM proteins are expressed and play significant roles in the testis. In the present study, we examined the spatiotemporal expression of ERM proteins in the mouse testis by Western blotting and immunohistochemistry. Ezrin immunoreactivity was demonstrated in the cytoplasm of steps 15 and 16 spermatids from 5 weeks postpartum through adulthood, whereas radixin immunoreactivity was in the apical cytoplasm of Sertoli cells from 1 week through 2 weeks postpartum. No immunoreactivity for moesin was detected at any age. Immunoprecipitation demonstrated that ezrin was bound to the cytoskeletal component actin, whereas radixin was bound to both actin and tubulin. Of the transmembrane proteins known to interact with ERM proteins, only cystic fibrosis transmembrane conductance regulator, a chloride transporter, was bound to ezrin in elongated spermatids. These results suggest that ezrin is involved in spermiogenesis whereas radixin is involved in the maturation of Sertoli cells, through interaction with different sets of membrane proteins and cytoskeletal components. (*J Histochem Cytochem* 57:351–362, 2009)

KEY WORDS

immunohistochemistry
Western blotting
immunoprecipitation
RT-PCR
mouse spermiogenesis
spermatids
Sertoli cells
ERM
CFTR
cytoskeleton

SPERMATOGENESIS IS THE PROCESS through which highly differentiated spermatozoa are produced from spermatogenic cells. In seminiferous tubules, spermatogonia located at the bottom of the basal compartment go up along the surface of Sertoli cells while differentiating through the steps of spermatocyte and spermatid to reach the top of the adluminal compartment (Kerr et al. 2006). In the haploid phase of spermatogenesis, i.e., spermiogenesis, spermatids undergo extensive changes in shape to become mature sperms. During postnatal development of the testis, maturation of Sertoli cells proceeds, and the blood–testis barrier is formed around 2 weeks (Griswold and McLean 2006). The seminiferous epithelium, composed only of Sertoli cells and pro-spermatogonia at birth (Burgoyne 1987),

begins the first wave of spermatogenesis at 6 days postpartum (Bellvé et al. 1977) and completes it by 35 days postpartum (Kramer and Erickson 1981). These changes in cellular composition, location, and shape in the seminiferous epithelium during postnatal development of the testis and in adult spermatogenesis implicate roles of membrane proteins and cytoskeletal components. Both spermatogenic and Sertoli cells possess many types of membrane proteins, including hormone and cytokine receptors, ion channels, transporters, and cell adhesion molecules. On the inside of the plasma membrane, such transmembrane proteins interact with cytoskeletal components through adaptor proteins, which act as connecting molecules in signal transduction pathways (Pawson and Scott 1997). Among the adaptor proteins, α -, β -, and γ -catenins and zyxin have been documented in the testis. β -Catenin or γ -catenin structurally interacts with *N*- and *E*-cadherin and links them to the actin filament through α -catenin at the junction between adjacent Sertoli cells that forms the blood–testis barrier (Wong and Cheng 2005). Zyxin is another adaptor protein associated with the

Correspondence to: Tomohiko Wakayama, MD, PhD, Department of Histology and Embryology, Graduate School of Medical Science, Kanazawa University, 13-1 Takara-machi, Kanazawa, Ishikawa, 920-8640, Japan. E-mail: twaka@basic.m.kanazawa-u.ac.jp

Received for publication August 6, 2008; accepted November 24, 2008 [DOI: 10.1369/jhc.2008.952440].

actin filament and is found at the focal contact and leading edge of the cytoplasmic process of Sertoli cells (Lee et al. 2004).

The ezrin, radixin, and moesin (ERM) proteins represent a family of adaptor proteins that plays key roles in cell morphology, motility, signal transduction, and apoptosis (Vaheri et al. 1997; Mangeat et al. 1999). In cultured cell systems, ERM proteins are located at cell surface structures such as apical microvilli, filopodia, ruffling membranes, retraction fibers, and the cleavage furrow of dividing cells, and at adhesion sites, where actin filaments are associated with the plasma membrane. ERM proteins are capable of binding to a variety of transmembrane proteins and to F-actin through their N- and C-terminal domains, respectively, thereby regulating dynamic changes of the membrane-cytoskeleton interaction (Turunen et al. 1994). The activity of ERM proteins undergoes conformational regulation. Inactivation of ERM proteins occurs when intramolecular and intermolecular association of the N- and C-terminal domains causes mutual suppression of their membrane- and actin-binding activities. ERM proteins have been shown to join actin filaments to a variety of transmembrane proteins, including cell adhesion molecules such as CD43, CD44 (Yonemura et al. 1998), CD95 (Parlato et al. 2000), syndecan-2 (Granés et al. 2000), and intercellular adhesion molecule-1 (ICAM-1) (Heiska et al. 1998), ICAM-2 (Yonemura et al. 1998), and ICAM-3 (Serrador et al. 2002), as well as membrane channels and receptors such as Na⁺/H⁺ exchanger-3 (NHE3) (Yun et al. 1998), multidrug-resistance protein 2 (Mrp2) (Kikuchi et al. 2002), cystic fibrosis transmembrane conductance regulator (CFTR) (Short et al. 1998), and the β 2-adrenergic receptor (Adrb2) (Tsukita and Yonemura 1999).

Ezrin was the first member of the ERM proteins isolated as a component of chicken intestinal microvillus cytoskeleton (Bretscher 1983), radixin was originally identified as a molecule involved in adherence junctions in rat liver (Tsukita et al. 1989), and moesin was originally identified as a heparin-binding protein abundant in bovine smooth-muscle cells of the uterus (Lankes and Furthmayr 1991). In the adult mouse *in vivo*, ezrin is expressed in absorptive epithelial cells of the intestine, pigment epithelial and Müller cells of the retina, and gastric parietal cells, where it is enriched at the apical surface (Saotome et al. 2004; Tamura et al. 2005; Bonilha et al. 2006). Radixin is mainly present in the cell-to-cell adherens junction of hepatocytes (Tsukita et al. 1989) and is also enriched in cochlear stereocilia (Kitajiri et al. 2004; Pataky et al. 2004). Moesin is found primarily in endothelial cells (Lankes and Furthmayr 1991). Ezrin knockout (KO) mice show abnormal morphogenesis in the gastrointestinal epithelia, resulting in postnatal death (Saotome et al. 2004). Radixin KO mice are characterized by a disorder of

the apical microvilli of hepatocytes, resulting in liver injury after 8 weeks postpartum, similar to human conjugated hyperbilirubinemia in Dubin-Johnson syndrome (Kikuchi et al. 2002). On the other hand, moesin KO mice have no apparent defects (Doi et al. 1999). However, it remains unknown whether ERM proteins are expressed and play significant roles in the testis.

In the present study, we examined expression and localization of the ERM proteins as well as interaction of the ERM proteins with transmembrane and cytoskeletal proteins in the adult and postnatal mouse testes, using Western blotting, immunohistochemistry, and immunoprecipitation.

Materials and Methods

Animals and Tissue Preparation

Male Slc:ddY mice at postnatal ages 1–6 weeks and at 10 weeks (adult) and female Wistar rats at 8 weeks were purchased from Nippon SLC, Inc. (Hamamatsu, Japan). They were raised under standard laboratory conditions with a 12-hr light/12-hr dark cycle and free access to food and water. All subsequent animal experiments were performed according to the Guidelines for the Care and Use of Laboratory Animals at Kanazawa University. The animals were anesthetized with an intraperitoneal injection of sodium pentobarbital (50 mg/kg) and sacrificed by bleeding from the right atrium, followed by transcardial perfusion with cold physiological saline. To isolate total RNA for RT-PCR or to make cell lysates for Western blotting and immunoprecipitation, the testes were dissected out, frozen immediately in liquid nitrogen, and stored at –80C until use. To make tissue sections for immunohistochemistry, the animals were fixed by perfusion with cold 4% paraformaldehyde in 0.1 M phosphate buffer (pH 7.2), and the testes were dissected out. They were further fixed by immersion in the same fixative overnight at 4C, rinsed overnight at 4C with 30% sucrose in 0.1 M phosphate buffer, and then frozen and cut into 8- μ m sections using a cryostat. The sections were mounted on silanized glass slides (DAKO; Glostrup, Denmark).

Preparation of Primary Antibodies

Rabbit polyclonal anti-ezrin (H-276 and H-300), anti-ICAM-1 (M-19), anti-syndecan-2 (M-140), goat polyclonal anti-CFTR (N-20), and anti-moesin (C-15) antibodies were purchased from Santa Cruz Biotechnology (Santa Cruz, CA). Rat monoclonal anti-radixin (clone R21) antibody was from Sanko Junyaku (Tokyo, Japan), and mouse monoclonal anti- α -tubulin (clone DM 1A) and anti- β -actin (clone AC-15) antibodies were from Sigma-Aldrich (St. Louis, MO). Rat polyclonal antisera against mouse radixin and moesin were produced in our laboratory according to the method de-

scribed previously, with a modification (Wakayama et al. 2006). Briefly, cDNA fragments 123 bp in length coding the carboxyl-termini of mouse radixin and moesin, respectively, were cloned into the bacterial expression vector pGEX-6p-1 (Amersham Pharmacia Biotech; Uppsala, Sweden). By introducing these vectors into the bacteria BL21 (Novagen; Madison, WI), recombinant oligopeptides 41 amino acids in length for radixin and moesin, respectively, fused with the carrier protein glutathione-S-transferase, were produced. They were then emulsified with Freund's complete adjuvant and injected as antigens into footpads of Wistar rats. A booster immunization was made 2 weeks later, and sera were collected 1 week after the booster.

Western Blot Analysis

Western blotting was performed as previously described (Wakayama et al. 2007). Twenty- μ g aliquots of cell lysate from the mouse testis were subjected to SDS-PAGE and transferred to polyvinylidene difluoride membranes (Bio-Rad Laboratories; Hercules, CA). The blots were incubated with one of the following primary antibodies: rabbit polyclonal anti-ezrin antibodies (H-276 and H-300) (0.5 μ g/ml), rat monoclonal anti-radixin antibody (0.5 μ g/ml), rat polyclonal anti-radixin antisera (1:1000), goat polyclonal anti-moesin antibody (1 μ g/ml), rat polyclonal anti-moesin antisera (1:1000), or mouse monoclonal anti- α -tubulin antibody (1:2000). After being washed, the blots were further incubated with one of the horseradish peroxidase-labeled secondary antibodies against rabbit, rat, goat, and mouse IgG (DAKO) at 1:5000 dilution. The immunoreaction was detected with X-ray film after treatment of the blots with the chemiluminescent reagent ECL-plus (Amersham Pharmacia Biotech).

Immunohistochemistry

Immunohistochemistry at the light microscopic level was performed as previously described (Wakayama et al. 2007). Briefly, the 4% paraformaldehyde-fixed frozen sections of the mouse testis were first treated with 5% normal goat serum to prevent nonspecific antibody binding and then incubated overnight at 4C with one of the following primary antibodies: rabbit polyclonal anti-ezrin antibodies (H-276 and H-300) (2 μ g/ml), rat monoclonal anti-radixin antibody (1 μ g/ml), rat polyclonal anti-radixin antisera (1:800), and goat polyclonal anti-CFTR antibody (2 μ g/ml). For negative control, normal rabbit IgG (DAKO) (2 μ g/ml), normal rat IgG (1 μ g/ml), and normal goat IgG (1 μ g/ml) were used in place of the primary antibodies. After the sections were washed in PBS, the immunoreaction was visualized by incubating the sections with anti-rabbit IgG antibody conjugated with Alexa Fluor 488 or 594 (Molecular Probes; Eugene, OR) at 1:400, anti-rat IgG

antibody conjugated with Alexa Fluor 594 at 1:400, or anti-goat IgG antibody conjugated with Alexa Fluor 488 at 1:400 for 1 hr at room temperature. The sections were counterstained in the nucleus with bisbenzimidazole H33258 (Hoechst 33258) (Sigma-Aldrich) at 100 ng/ml. They were then subjected to observation with an immunofluorescence microscope (BX50/BX-FLA; Olympus, Tokyo, Japan) or with a confocal laser scanning microscope (LSM510; Carl Zeiss, Oberkochen, Germany).

For ultrastructural localization of ezrin and radixin in the mouse seminiferous epithelium, the pre-embedding immunoelectron microscopy was performed as described previously (Wakayama et al. 2003a,b; Tsukioka et al. 2007). The cryostat sections of testes were first treated with 5% normal horse serum for 30 min to prevent nonspecific antibody binding and then incubated overnight at 4C with rabbit polyclonal anti-ezrin antibody (H-276) or rat monoclonal anti-radixin antibody. After the sections were washed in PBS, the sites of immunoreaction were visualized by incubating the sections successively with biotinylated horse anti-rabbit IgG or horse anti-rat IgG antibody (Vector Laboratories; Burlingame, CA) for 1 hr, horseradish peroxidase-conjugated streptavidin (DAKO) for 1 hr, and 3'3'-diaminobenzidine tetrahydrochloride solution (Dojin; Osaka, Japan) containing H₂O₂ for a few minutes. The sections were then fixed with 1% OsO₄, stained with 1% uranyl acetate, and embedded in Glicidether (Selva Feinbiochemica; Heidelberg, Germany). Ultrathin sections were prepared using an ultramicrotome and subjected to observation with a JEM-1210 electron microscope (JEOL; Tokyo, Japan).

Immunoprecipitation Analysis

Immunoprecipitation was performed as described previously (Wakayama et al. 2007). Cell lysate from the 2-week-old or 10-week-old mouse testis containing 200 μ g of protein was preabsorbed with protein-G-agarose (Roche Diagnostics; Mannheim, Germany) for at least 3 hr at 4C. After centrifugation, the supernatant was incubated with rabbit polyclonal anti-ezrin antibody (H-276 or H-300) (10 μ g/ml), rat monoclonal anti-radixin antibody (10 μ g/ml), or rat polyclonal anti-radixin antisera (1:40) for 2 hr and further incubated with protein-G-agarose for at least 3 hr at 4C. For negative control, reaction with normal rabbit or rat IgG (10 μ g/ml) was also performed. After centrifugation, the immunoprecipitated product was washed and resuspended in the sample buffer for SDS-PAGE. Cell lysate from the mouse testis and the immunoprecipitated products were then subjected to Western blot analysis as described above, using rabbit polyclonal anti-ezrin antibody (H-276 or H-300) (0.5 μ g/ml), rat monoclonal anti-radixin antibody (0.5 μ g/ml), rat polyclonal anti-radixin antisera (1:1000), goat poly-

clonal anti-CFTR antibody (0.5 $\mu\text{g/ml}$), or rabbit polyclonal anti-syndecan-2 antibody (0.5 $\mu\text{g/ml}$).

RNA Preparation and RT-PCR

Total RNA was isolated from the 2-week-old and 10-week-old testes by using an acid guanidine-based solution (TRI Reagent; Sigma-Aldrich). First-strand cDNA was synthesized from a 1- μg aliquot of the total RNA samples using the oligo-dT primer and reverse transcriptase (RevertraAce; Toyobo, Osaka, Japan). Using these RT products, RT-PCR was performed for 28 cycles using DNA polymerase (Blend Taq; Toyobo) and the primer pairs for various membrane proteins known to interact with ERM proteins in a DNA thermal cycler (96-well GeneAmp PCR System 9700; Applied Biosystems, Foster City, CA), and the amplified products were analyzed with agarose gel electrophoresis. The sequences of the primers used are shown in Table 1.

Results

Expression of ERM Proteins in the Mouse Testis

We performed Western-blot analysis using anti-ezrin, anti-radixin, and anti-moesin antibodies and the cell lysates obtained from the testes of postnatal developing and adult (10-week) mice (Figure 1). The immunoreactive band for ezrin, with a molecular mass of 85 kDa, appeared first at 5 weeks and subsequently maintained

the same intensity and size until 10 weeks, whereas the immunoreactive band for radixin, with a molecular mass of 82 kDa was detected at 1 week through 2 weeks but disappeared by 3 weeks. On the other hand, no immunoreactive band for moesin, with a molecular mass of 75 kDa, was detected at any age. In the stomach, liver, and uterus, which are known to express ERM proteins (Tsukita et al. 1989; Lankes and Furthmayr 1991; Tamura et al. 2005), intense bands with molecular mass corresponding to ezrin, radixin, and moesin, respectively, were obtained. Furthermore, pairs of two different antibodies against ezrin, radixin, and moesin, as described in Materials and Methods, all produced the same results.

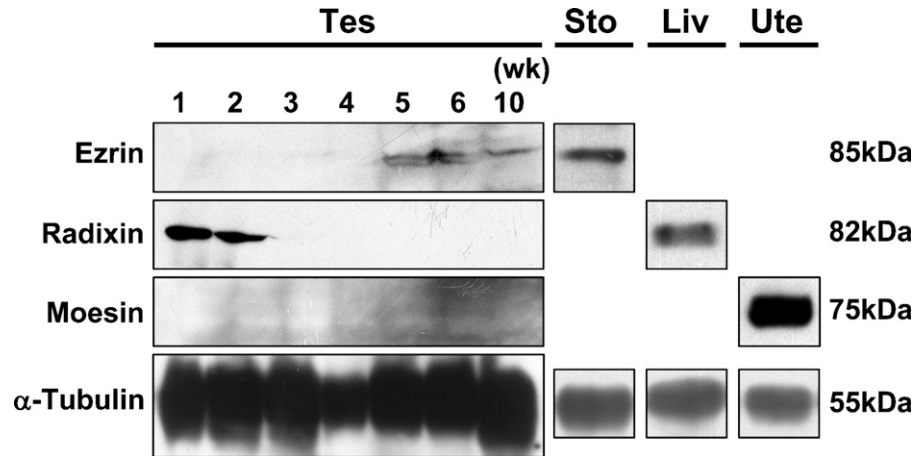
Immunohistochemical Localization of Ezrin in the Adult Mouse Testis

To examine the cellular localization of ezrin, we performed immunohistochemistry in frozen sections of the adult mouse testis (Figure 2). Immunostaining for ezrin was found exclusively in the seminiferous tubules and was not detected in the interstitial tissue (Figure 2A). There was a marked difference in the intensity of the immunostaining among tubular sections in different stages of the spermatogenesis. Incubation with normal rabbit IgG showed no immunostaining (Figure 2B). In the seminiferous epithelia, the immunopositive cells were found close to the lumen and represented elongated spermatids. Using the staging criteria for mouse spermatogenesis (Russell et al. 1990), the strong immunoreactivity for ezrin was localized to the step 15–16 spermatids present in the stage IV–VIII epithelia (Figures 2D and 2E), whereas it was absent in the step 14 spermatids present in the stage II–III epithelia (Figure 2C). The strong immunoreactivity was also present in residual bodies representing the cytoplasm removed from mature sperms by spermiation in the stage IX epithelium (Figure 2F). No immunoreactivity was recognized in other spermatids (steps 1–13), spermatocytes, spermatogonia, or Sertoli cells. Also, the mature sperms in the epididymis were negative for ezrin immunoreactivity (data not shown). Furthermore, subcellular localization of ezrin was examined in the stage VI seminiferous epithelium with pre-embedding immunoelectron microscopy (Figures 2G and 2H). On the top of the epithelium were the step 15 spermatids, characterized by their elongated nuclei with condensed chromatin and flagella with well-developed axonema. The high electron density representing the immunoreactivity for ezrin was localized primarily in the cytoplasm surrounding the axonema of these elongated spermatids. No immunoreactivity was detected in the round spermatids at step 6 or Sertoli cells. We also performed immunohistochemistry for ezrin in the testes from postnatal developing mice. Immunoreactivity was not

Table 1 Specific primers used for RT-PCR analyses

Gene	Primers	Sequence
Adrb2	Forward	5'-TCCACGCCAAAACCTCAGC-3'
	Reverse	5'-CCTTCCTTGGGAGTCAACGC-3'
CD43	Forward	5'-GTGGCACCTCAGTTCCAGC-3'
	Reverse	5'-TGTGGACCGTCAGAAGTTGG-3'
CD44	Forward	5'-TGACCCTGCTAAAACCTGAGGT-3'
	Reverse	5'-CCCCAATCTTCATGTCCACACT-3'
CD95	Forward	5'-CGCCTCGTGTGAACATGGAA-3'
	Reverse	5'-TCCTTCTGGACCATGTCCTG-3'
CFTR	Forward	5'-GAGGGTGGGGCTCTTAGGAA-3'
	Reverse	5'-CGCTGGCAATCCAACATCGC-3'
ICAM-1	Forward	5'-CTGTGAAGTGTGAAGCCAC-3'
	Reverse	5'-CATAAGAGGCTGCCATCACG-3'
ICAM-2	Forward	5'-GGAAAGCAGCACTCGGAGAG-3'
	Reverse	5'-CGTAGGTGCCTGTCCGCTT-3'
ICAM-3	Forward	5'-CGAAGGGATAGTGTGGCCCT-3'
	Reverse	5'-CCACGCTCAGAGTGTATTG-3'
Mrp2	Forward	5'-CTCCGGCAGATTGCCAAA-3'
	Reverse	5'-GAACTCGTCCGGATGGTCG-3'
NHE3	Forward	5'-CGGCACGAGTAACACCCAA-3'
	Reverse	5'-GCGGAAGTTGCTGGAGAGT-3'
Syndecan-2	Forward	5'-CCTGCTCACCTTGGGCTTGA-3'
	Reverse	5'-GTGGGTGCCTTCTGGTAAGC-3'
GAPDH	Forward	5'-ACCACAGTCCATGCCATCAC-3'
	Reverse	5'-TCCACCACCTGTTGCTGTA-3'

Figure 1 Western blot analysis for ezrin, radixin, and moesin in the adult and developing mouse testis. The cell lysates of the testes (Tes) from mice at 1–6 weeks and 10 weeks were electrophoresed in polyacrylamide gel, blotted onto polyvinylidene difluoride membrane, and stained with rabbit polyclonal anti-ezrin (H-276) antibody, rat monoclonal anti-radixin (R21) antibody, rat polyclonal anti-moesin antisera, or mouse monoclonal anti- α -tubulin antibody. For positive control, the same antibodies were applied to the cell lysates of the stomach (Sto), liver (Liv), and uterus (Ute) from adult mice. The molecular mass (kDa) of the immunoreactive bands is indicated.



detected in any cell types from 1 week through 4 weeks, but was localized to the step 15 and 16 elongated spermatids after their first appearance in the seminiferous epithelium around 5 weeks (Kramer and Erickson 1981) (data not shown). Two different antibodies against ezrin (H276 and H300) produced the same result.

Immunohistochemical Localization of Radixin in the Developing Mouse Testis

The cellular localization of radixin was examined with immunohistochemistry in frozen sections of the testes from mice at 1 and 2 weeks postpartum (Figure 3). In the 1-week testis, in which only spermatogonia and Sertoli cells were present (Burgoyne 1987), immunostaining for radixin with moderate intensity was found in the center of all seminiferous tubules (Figure 3A). Incubation with normal rat IgG showed no immunostaining (Figure 3B). In the 2-week testis, the lumen had been formed in the center of seminiferous tubules, and the primary spermatocytes with a round shape and a large nucleus had appeared in the adluminal compartment of the seminiferous epithelium, consistent with the literature (Bellvé et al. 1977). Immunoreactivity was observed diffusely in the apical epithelial regions facing the lumen, suggesting that it belongs to Sertoli cells (Figures 3C and 3D). Furthermore, subcellular localization of radixin in the seminiferous epithelium of 2-week mouse testis was examined with pre-embedding immunoelectron microscopy (Figure 3E). The epithelium was composed of Sertoli cells, which are characterized by their clear triangular nuclei with distinct nucleoli, and primary spermatocytes, which are characterized by their large round nuclei located above the nuclei of Sertoli cells (Bellvé et al. 1977). The immunoreactivity for radixin was localized primarily to the apical cytoplasmic regions of Sertoli cells ranging from the luminal surface to the portions surrounding spermatocytes. In contrast, spermatocytes, as well as spermatogonia located at the base of the epithelium, were devoid of

immunoreaction for radixin. We also performed immunohistochemistry for radixin in the testes from adult mice and mice postnatal ages 3 to 6 weeks, but failed to detect any immunoreactivity in any cell type (data not shown). Two different antibodies against radixin (rat monoclonal and rat polyclonal antibodies) produced the same result.

Interaction of Ezrin and Radixin With Cytoskeletal Components

The cell lysates of adult (10-week) and 2-week testes were immunoprecipitated with anti-ezrin and anti-radixin antibodies, respectively, and the precipitated products as well as the cell lysates were analyzed with Western blotting using antibodies against ezrin, radixin, β -actin, and α -tubulin (Figure 4). Anti-ezrin antibody reacted with the cell lysate of adult testis as well as the anti-ezrin-precipitated product and formed an 85-kDa band, indicating that immunoprecipitation was performed properly (Figure 4A). Anti- β -actin antibody formed a 42-kDa-immunoreactive band not only in the cell lysate but also in the anti-ezrin-precipitated product, suggesting that ezrin is bound to β -actin in the cell lysate. In contrast, anti- α -tubulin antibody formed a 55-kDa band in the cell lysate but not in the ezrin-precipitated product, suggesting that ezrin is not bound to α -tubulin. Anti-radixin antibody reacted with the cell lysate of 2-week testis as well as the anti-radixin-precipitated product and formed an 82-kDa band, indicating that immunoprecipitation was performed properly (Figure 5B). Anti- β -actin and anti- α -tubulin antibodies formed corresponding immunoreactive bands not only in the cell lysate but also in the anti-radixin-precipitated product, suggesting that radixin is bound to both β -actin and α -tubulin. The immunoprecipitation products of adult and 2-week testes with normal rabbit IgG formed no band with any antibodies. Pairs of two different antibodies against ezrin and radixin both produced the same results.

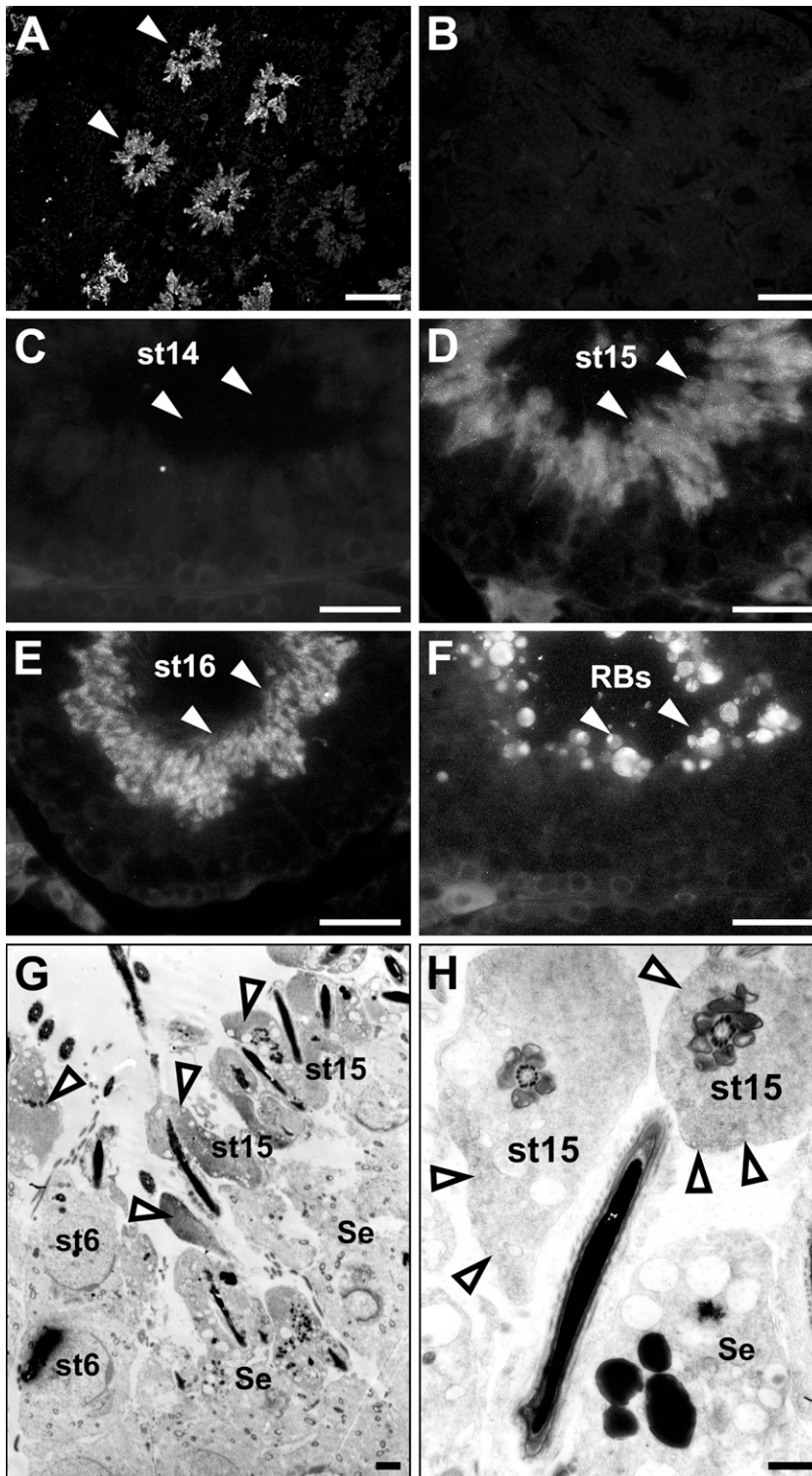


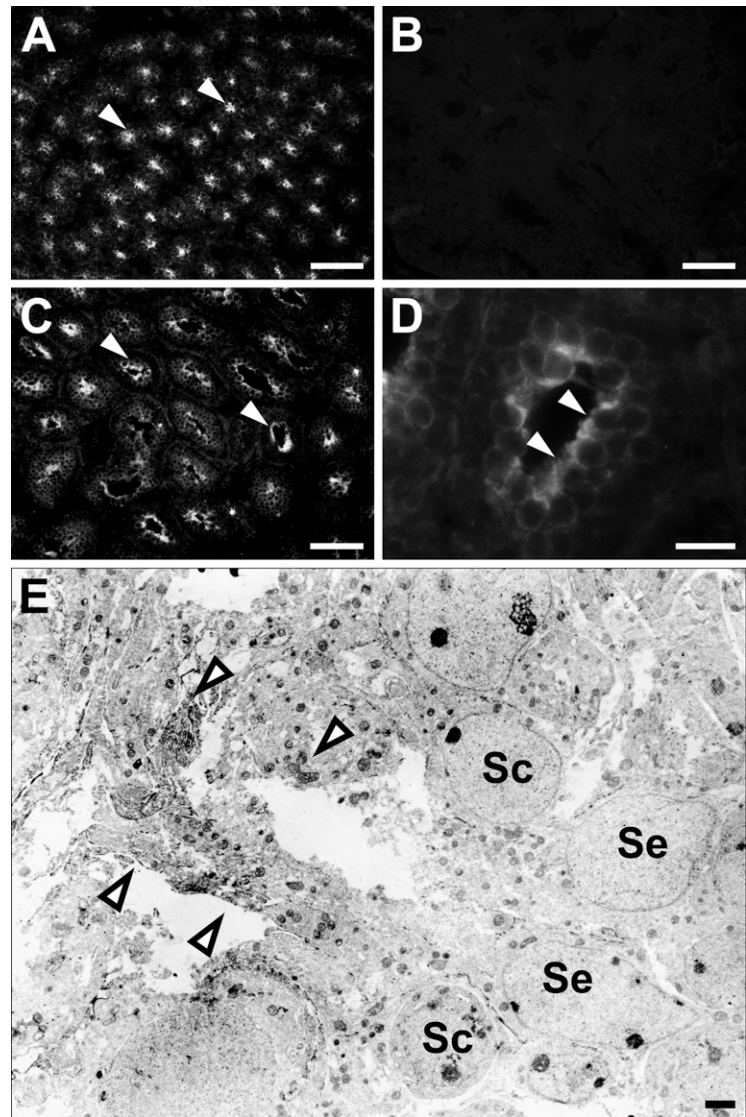
Figure 2 Immunohistochemistry showing the localization of ezrin in the adult mouse testis. The frozen sections of 10-week testis were immunostained with rabbit polyclonal anti-ezrin antibody (H-276) (A,C-H) or normal rabbit IgG (B) and observed with fluorescence (A-F) or electron (G,H) microscope. (A) Various patterns of ezrin immunoreactivity (arrowheads) are present in the seminiferous tubules in different stages. (B) No reactivity is present in any portions. (C) At stage II, no immunoreactivity (arrowheads) is present in the spermatids of step 14 (st14). (D) At stages IV–VI, the immunoreactivity (arrowheads) is localized in the spermatids of step 15 (st15). (E) At stage VIII, the immunoreactivity (arrowheads) is localized in the spermatids of step 16 (st16). (F) At stage IX, the immunoreactivity (arrowheads) is localized in the residual bodies (RBs). (G,H) Results of immunoelectron microscopy in the stage VI tubule. (G) In the spermatids of step 15, the immunoreactivity (arrowheads) is primarily localized in the cytoplasm. No immunoreactivity is present in the spermatids of step 6 (st6) or Sertoli cells (Se). (H) Higher magnification of the immunopositive spermatids of step 15 (st15) in G. Bars: A,B = 100 μ m; C-F = 25 μ m; G,H = 1 μ m.

Interaction of Ezrin With Cystic Fibrosis Transmembrane Conductance Regulator

We analyzed the total RNA of 2-week-old and 10-week-old mouse testes with RT-PCR for expression

of various membrane proteins known to interact with ERM proteins (Figure 5). Expression of cystic fibrosis transmembrane conductance regulator (CFTR) and syndecan-2 was detected in both the 2-week and

Figure 3 Immunohistochemistry showing the localization of radixin in the developing mouse testis. The frozen sections of 1-week (A,B) or 2-week (C-E) mouse testis were immunostained with rat monoclonal anti-radixin antibody (A,C-E) or normal rat IgG (B) and observed with fluorescence (A-D) or electron (E) microscope. (A) At 1 week, many seminiferous tubules display radixin immunoreactivity (arrowheads). (B) No immunoreactivity is present in any cells. (C) At 2 weeks, the immunoreactivity (arrowheads) is localized in the region facing the lumen of seminiferous tubules. (D) Higher magnification of the tubule in C. (E) Result of immunoelectron microscopy in the 2-week tubule. The immunoreactivity (arrowheads) is primarily localized in the apical cytoplasmic portions of Sertoli cells (Se). No immunoreactivity is present in spermatocytes (Sc). Bars: A-C = 50 μ m; D = 25 μ m; E = 1 μ m.



10-week testes, and of intercellular adhesion molecule-1 (ICAM-1) in the 2-week testis, whereas expression of other membrane proteins, such as ADRB2, CD43, CD44, CD95, ICAM-2, ICAM-3, Mrp2, and NHE3, was not detected in 2-week or 10-week testis. We then examined whether ezrin and radixin interact with CFTR and syndecan-2 in the testis using immunoprecipitation and Western blotting (Figure 6). The cell lysates of adult (10-week) and 2-week testes were immunoprecipitated with anti-ezrin and anti-radixin antibodies, respectively, and the precipitated products as well as the cell lysates were analyzed with Western blotting using antibodies against CFTR and syndecan-2. Anti-CFTR antibody formed a 165-kDa-immunoreactive band not only in the cell lysate of 10-week testis but also in the anti-ezrin-precipitated product, suggesting that ezrin is bound to CFTR in the testis. No immunoreactive

band was formed in either the cell lysate of 2-week testes or the anti-radixin-precipitated product. In contrast, anti-syndecan-2 antibody detected a 22-kDa-immunoreactive band in the cell lysates of both 10-week and 2-week testes but not in the anti-ezrin- or anti-radixin-precipitated product, suggesting that syndecan-2 is bound to neither ezrin nor radixin. Double-immunofluorescence microscopy further demonstrated colocalization of ezrin and CFTR in step 15 elongated spermatids in the stage VI adult seminiferous epithelium, reinforcing the notion that ezrin interacts with CFTR in the elongated spermatid (Figure 7). Two different antibodies against ezrin produced the same result. As for ICAM-1, the mRNA of which was detected in the 2-week testis, we performed Western blot analysis using anti-ICAM-1 antibody but failed to detect an immunopositive band in the cell lysate of

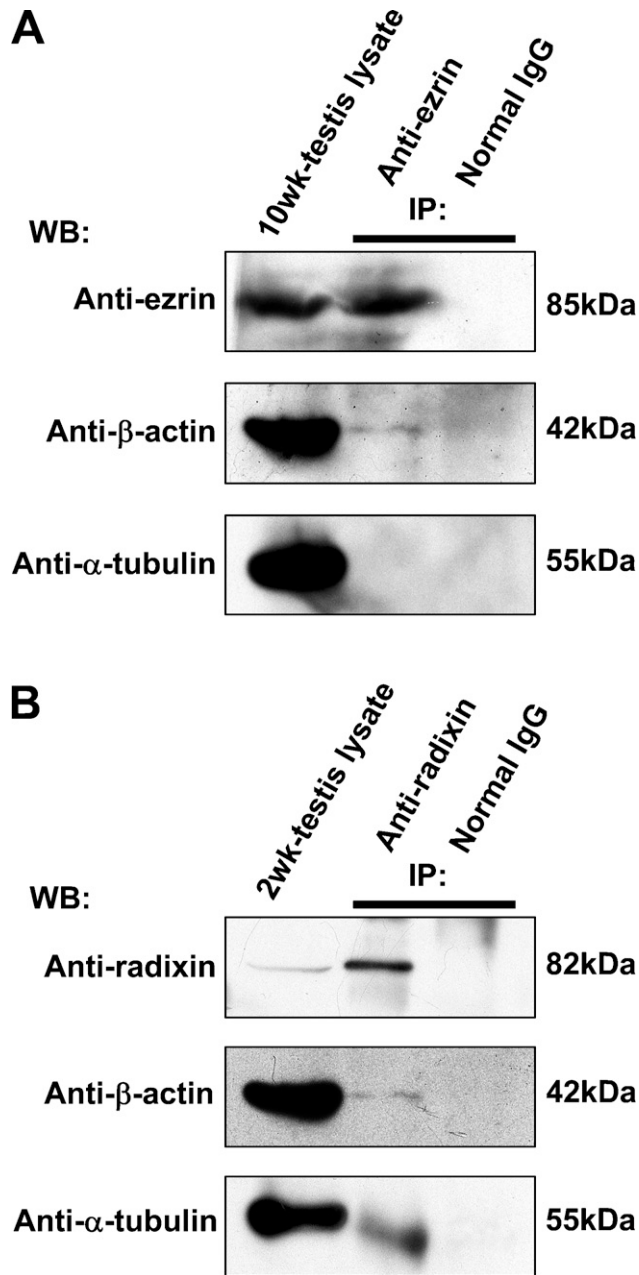


Figure 4 Immunoprecipitation (IP) analysis in the adult and 2-week mouse testes for the interaction of ezrin and radixin with β -actin and α -tubulin. (A) IP was performed in the cell lysate of the 10-week testis using rabbit polyclonal anti-ezrin antibody (H-276) or normal rabbit IgG. The testis lysate and products of IP were analyzed with Western blotting (WB) using anti-ezrin, anti- β -actin, or anti- α -tubulin antibody. (B) IP was performed in the cell lysate of the 2-week testis using rat monoclonal anti-radixin antibody or normal rat IgG. The testis lysate and products of IP were analyzed with WB using anti-radixin, anti- β -actin, or anti- α -tubulin antibody. The molecular mass (kDa) of the immunopositive bands is indicated.

2-week or 10-week testis (data not shown). However, immunohistochemistry using the same antibody showed immunoreactivity localized exclusively to vascular endothelial cells in both the 2-week and 10-week testes

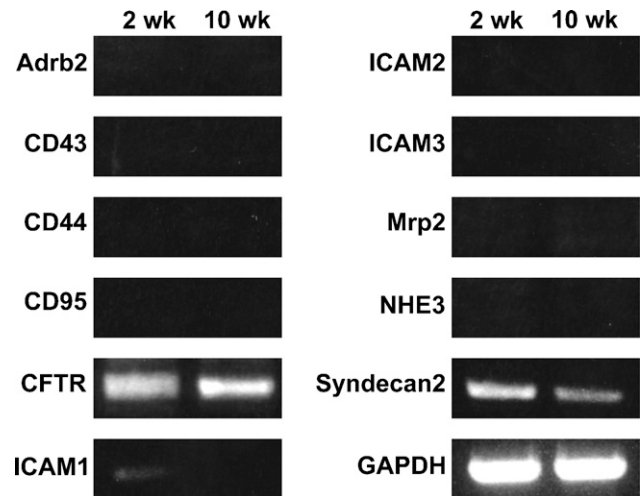


Figure 5 RT-PCR analysis showing the expression of various membrane proteins in the 2- and 10-week mouse testes. Amplified products from the total RNA of 2- and 10-week testes were electrophoresed and stained with ethidium bromide. Expression of GAPDH is for the positive control.

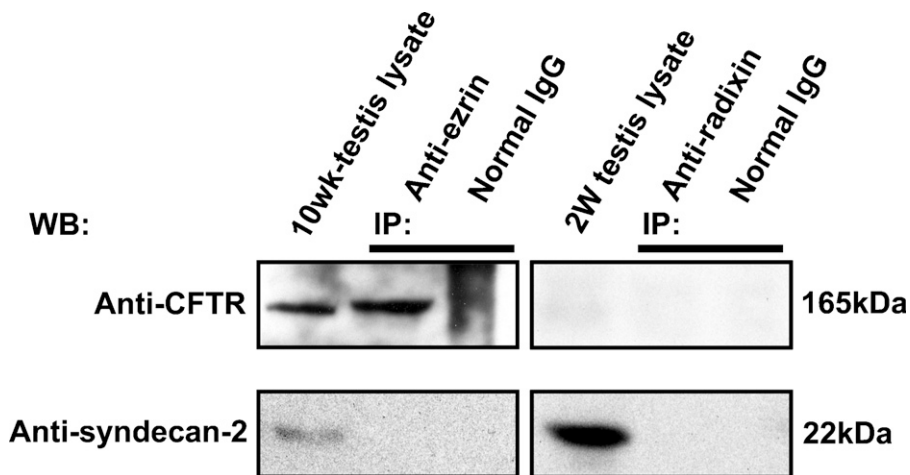
(data not shown), consistent with the literature (Smith and Thomas 1990).

Discussion

In the present study, we have provided evidence for the expression of ezrin and radixin, but not moesin, in the mouse testis by Western blotting and immunohistochemistry. Ezrin and radixin have shown strikingly different spatiotemporal expression patterns, with ezrin expressed in elongated spermatids from 5 week postpartum to adulthood, and radixin in Sertoli cells from 1 week through 2 weeks postpartum. The lack of expression of moesin in the testis has also been confirmed with RT-PCR (data not shown).

The elongated spermatid first appears in the mouse testis around 5 weeks of age at the end of the first wave of spermatogenesis (Bellvé et al. 1977), coincident with the occurrence of ezrin in the present Western blotting. Furthermore, the present immunohistochemical results indicate that ezrin is localized exclusively in the cytoplasm of step 15–16 elongated spermatids, which are located in the apical portions of the stage IV–VIII seminiferous epithelia. The cytoplasm of these spermatids undergoes a drastic decrease in volume, separates from the mature sperms in spermiation, and finally forms residual bodies in the stage IX seminiferous epithelium. Such a process of morphological changes in elongated spermatids is likely to involve participation of cytoskeletal components. The present results of double immunostaining and immunoprecipitation indicate that at least some of the ezrin molecules in elongated spermatids are bound to cytoplasmic actin. The relatively weak band for actin in the ezrin-immunoprecipitated

Figure 6 Immunoprecipitation (IP) analysis in the adult and 2-week mouse testes for the interaction of ezrin and radixin with cystic fibrosis transmembrane conductance regulator (CFTR) and syndecan-2. IP was performed in the cell lysate of the 10-week testis using rabbit polyclonal anti-ezrin antibody (H-276) or normal rabbit IgG, and in the cell lysate of the 2-week testis using rat monoclonal anti-radixin antibody or normal rat IgG. The testis lysates and the products of IP were analyzed with Western blotting (WB) using goat polyclonal anti-CFTR or rabbit polyclonal anti-syndecan-2 antibody. The molecular mass (kDa) of the immunopositive bands is indicated.



product shown in Figure 4 is not unexpected, taking into account that only part of the total cytoplasmic actin may form the actin filament, of which only part may be bound to the plasma membrane through a particular adaptor protein. The present results have further revealed CFTR as a candidate of the functional membrane protein bound to ezrin in elongated spermatids. Of the variety of transmembrane proteins known to bind ezrin, only CFTR has been reported to occur in the seminiferous epithelium of rat testis, where it is localized in the spermatids from steps 8 through 19 (corresponding to mouse spermatids from steps 8 through 16) (Gong et al. 2001). In the present study, we have confirmed co-localization of the immunoreactivity for CFTR and ezrin in the step 15–16 mouse elongated spermatids, as well as co-immunoprecipitation of CFTR and ezrin in the cell lysate of mouse testis, evidence for the interaction of CFTR and ezrin in elongated spermatids. CFTR is a cAMP-regulated ion channel protein that transports chloride ions across epithelial cell membranes in many organs, including the lung, liver, pancreas, digestive tract, reproductive tract, and skin (Kelley et al. 1992; Lewis et al. 2003). CFTR is known to form a complex with aquaporins, a water channel family, thereby regulating the excretory function of a variety of cells (Lewis et al. 2003). CFTR excretes chloride ions into the lumen of seminiferous tubules, whereas aquaporins function as both influx and efflux water channels. In the rat seminiferous epithelium, aquaporins 7 and 8 are known to occur, of which aquaporin 7 is localized to the plasma membrane of elongated spermatids and implicated in reduction of their cytoplasmic volume (Suzuki-Toyota et al. 1999; Calamita et al. 2001; Kageyama et al. 2001). Because the luminal fluid of seminiferous tubules is known to be hypertonic (Levine and Marsh 1971), the CFTR–aquaporin 7 complex may collaborate and function in pumping out the chloride-rich cytoplasmic fluid effectively against the osmotic gradient. Furthermore,

the present results suggest that cytoplasmic actin filaments linked by ezrin to the CFTR–aquaporin 7 complex play a role in the cytoplasmic volume reduction by retracting the plasma membrane in elongated spermatids during spermiogenesis. Unfortunately, because the ezrin KO mice die in the early postnatal ages because of digestive failure (Saotome et al. 2004), they cannot be used for evaluating this hypothesis on the physiological significance of ezrin in spermatogenesis.

During postnatal development of the mouse testis, Sertoli cells cease to proliferate and begin to mature by 2 weeks (Bellvé et al. 1977; Kluin et al. 1984). The blood–testis barrier, which is not present at birth, is formed around 10–16 days of age as a result of the formation of the Sertoli–Sertoli cell junction, composed of occluding and gap junctions near the basement membrane. This junctional complex is associated with an array of cytoplasmic actin filaments called the basal ectoplasmic specialization. Coincident with the barrier formation, a lumen appears in the center of the seminiferous tubules and begins to expand as a result of fluid secretion from Sertoli cells. Thereafter, the first wave of spermiogenesis takes place at around 20 days of age, which is associated with a marked elongation of Sertoli cells and formation of numerous surface projections of Sertoli cells that contact spermatogenic cells directly (Bellvé et al. 1977; Kluin et al. 1984). Such a process of morphological changes in the seminiferous epithelium around 2 weeks is likely to involve participation of cytoskeletal components in Sertoli cells. Sertoli cells possess three cytoskeletal components: the actin filament, the vimentin filament, and the microtubule (Vogl et al. 1993). Of these, microtubules are distributed in the apical cytoplasmic portions and implicated in the maintenance of cell shape and movement of intracellular organelles. The present results indicate that radixin occurs in the apical cytoplasmic portions of Sertoli cells proceeding to and around the critical age of 2 weeks. Unlike the case of ezrin, the

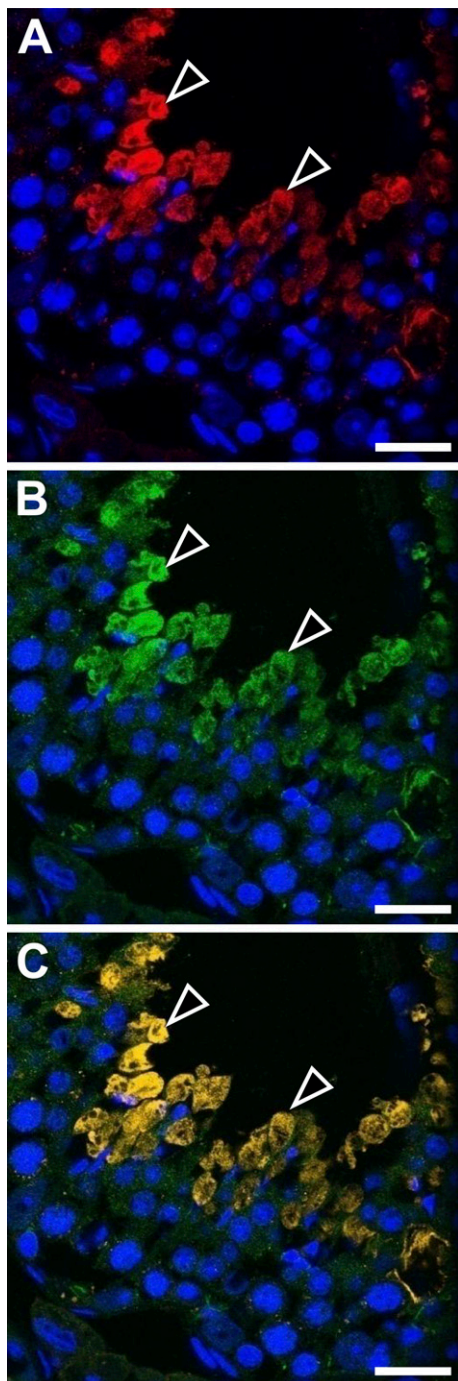


Figure 7 Double immunostaining in the stage VI seminiferous epithelium of adult mouse testis with rabbit polyclonal anti-ezrin (H-276) and goat polyclonal anti-CFTR antibodies observed with confocal laser microscope. The immunoreactivity (arrowheads) for ezrin (red, **A**) and for CFTR (green, **B**) overlaps in the step 15 spermatids when the images are merged (yellow, **C**). Bar = 25 μ m.

product of immunoprecipitation in testis lysates with anti-radixin antibody contains tubulin as well as actin. It is generally accepted that the ERM family molecules have no tubulin-binding site. However, there is evi-

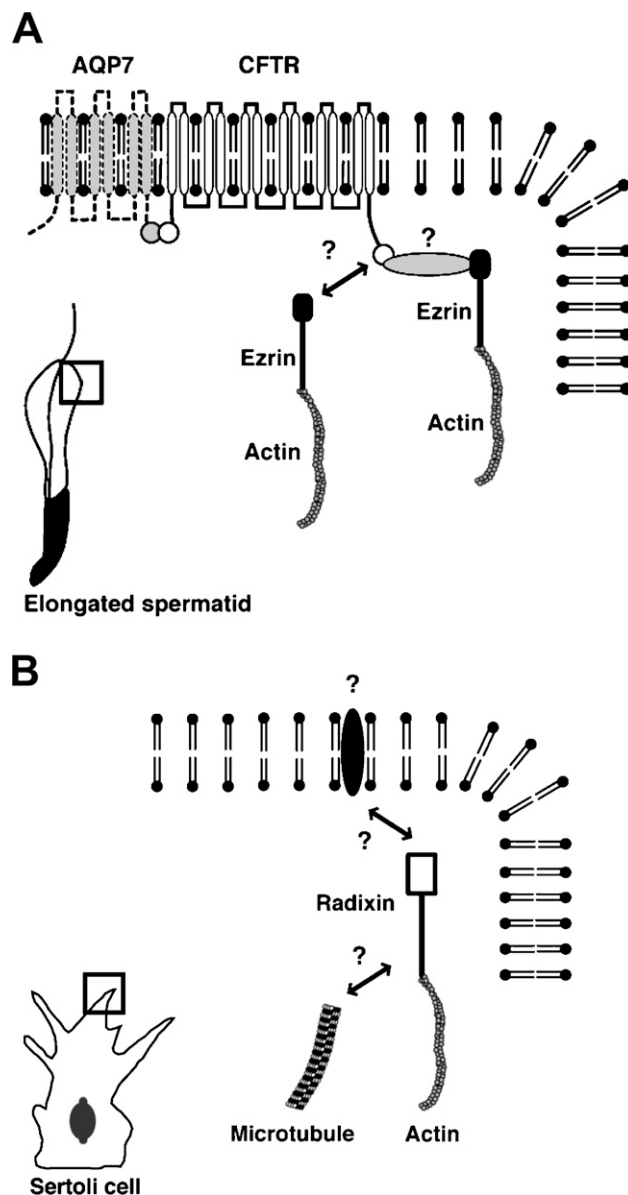


Figure 8 Schematic representations of the molecules that interact with ezrin in the elongated spermatid and with radixin in the developing Sertoli cell. (**A**) In the elongated spermatid, ezrin binds to actin filament in the cytoplasm and also binds directly or indirectly to CFTR, which interacts with aquaporin 7 (AQP7) in the plasma membrane. (**B**) In the developing Sertoli cell, radixin binds to actin filament and also directly or indirectly to microtubules in the cytoplasm. Radixin may also bind to an unidentified transmembrane protein.

dence suggesting that ezrin is one of the microtubule-associated proteins in various cell types (Shestakova et al. 1998; Woodward and Crouch 2001). It is possible that ERM proteins bind indirectly to tubulin through some intervening molecules. The present results of double immunostaining and immunoprecipitation have raised the possibility that radixin plays a role in the

maturation of Sertoli cells by binding not only to actin filaments but also to microtubules near the apical membrane. Because the radixin KO mice survive to reproductive age and show no apparent infertility (Kikuchi et al. 2002), the role of radixin in Sertoli cells, if any, may be dispensable. However, it remains to be clarified whether the radixin KO mouse has no retardation or abnormality in the development of seminiferous tubules.

The next question to be solved is identification of the binding partner of radixin in the membrane side. So far, only Mrp2, an efflux transporter for bile acids in hepatocytes, has been known as the transmembrane protein that binds radixin. Radixin KO mice show a liver injury similar to human Durbin-Johnson syndrome, probably due to dysfunction of Mrp2 (Kikuchi et al. 2002). However, as shown with RT-PCR in the present study, Mrp2 does not occur in the testis. Instead, cell adhesion molecules, such as those associated with the blood–testis barrier, appear to be strong candidates for the membrane proteins linked by radixin to the cytoskeletal components in Sertoli cells. Sertoli cells are known to express adhesion molecules such as cadherin, nectin-2, poliovirus receptor (PVR), junctional adhesion molecule-B, coxackie and adenovirus receptor, and integrin α 6 β 1 (Johnson and Boekelheide 2002; Mueller et al. 2003; Siu and Cheng 2004; Mirza et al. 2006; Wakayama et al. 2007). We have examined some of these molecules, namely, *N*-cadherin, *E*-cadherin, and PVR, with immunoprecipitation but failed to detect their binding activity with radixin in the cell lysate of 2-week mouse testis. As mentioned in Results, ICAM-1, an adhesion molecule, is expressed in the 2-week testis, but it is restricted to vascular endothelial cells and, therefore, cannot be a binding partner of radixin in Sertoli cells. Further study will be required to identify the unknown transmembrane protein in the developing Sertoli cells that is linked by radixin to the cytoskeletal components.

In conclusion, the present study suggests that in the mouse testis, ezrin is involved in spermiogenesis whereas radixin is involved in the maturation of Sertoli cells, through interaction with different sets of membrane proteins and cytoskeletal components (Figure 8).

Literature Cited

- Bellvé AR, Cavicchia JC, Millette CF, O'Brien DA, Bhatnagar YM, Dym M (1977) Spermatogenic cells of the prepuberal mouse. Isolation and morphological characterization. *J Cell Biol* 74:68–85
- Bonilha VL, Rayborn ME, Saotome I, McClatchey AI, Hollyfield JG (2006) Microvilli defects in retinas of ezrin knockout mice. *Exp Eye Res* 82:720–729
- Bretscher A (1983) Purification of an 80,000-dalton protein that is a component of the isolated microvillus cytoskeleton, and its localization in nonmuscle cells. *J Cell Biol* 97:425–432
- Burgoyne PS (1987) The role of the mammalian Y chromosome in spermatogenesis. *Development* 101(suppl):133–141
- Calamita G, Mazzone A, Bizzoca A, Svelto M (2001) Possible involvement of aquaporin-7 and -8 in rat testis development and spermatogenesis. *Biochem Biophys Res Commun* 288:619–625
- Doi Y, Itoh M, Yonemura S, Ishihara S, Takano H, Noda T, Tsukita S (1999) Normal development of mice and unimpaired cell adhesion/cell motility/actin-based cytoskeleton without compensatory up-regulation of ezrin or radixin in moesin gene knockout. *J Biol Chem* 274:2315–2321
- Gong XD, Li JC, Cheung KH, Leung GP, Chew SB, Wong PY (2001) Expression of the cystic fibrosis transmembrane conductance regulator in rat spermatids: implication for the site of action of antispermatogenic agents. *Mol Hum Reprod* 7:705–713
- Granés F, Urena JM, Rocamora N, Vilaró S (2000) Ezrin links syndecan-2 to the cytoskeleton. *J Cell Sci* 113:1267–1276
- Griswold MD, McLean D (2006) The Sertoli cell. In Neill JD, ed. *Knobil and Neill's Physiology of Reproduction*. 3rd ed. New York, Academic Press, 949–975
- Heiska L, Alftan K, Grönholm M, Vilja P, Vaheri A, Carpén O (1998) Association of ezrin with intercellular adhesion molecule-1 and -2 (ICAM-1 and ICAM-2). Regulation by phosphatidylinositol 4, 5-bisphosphate. *J Biol Chem* 273:21893–21900
- Johnson KJ, Boekelheide K (2002) Dynamic testicular adhesion junctions are immunologically unique. II. Localization of classic cadherins in rat testis. *Biol Reprod* 66:992–1000
- Kageyama Y, Ishibashi K, Hayashi T, Xia G, Sasaki S, Kihara K (2001) Expression of aquaporins 7 and 8 in the developing rat testis. *Andrologia* 33:165–169
- Kelley KA, Stamm S, Kozak CA (1992) Expression and chromosome localization of the murine cystic fibrosis transmembrane conductance regulator. *Genomics* 13:381–388
- Kerr JB, Loveland KL, O'Bryan MK, de Kretser DM (2006) Cytology of the testis and intrinsic control mechanisms. In Neill JD, ed. *Knobil and Neill's Physiology of Reproduction*. 3rd ed. New York, Academic Press, 827–947
- Kikuchi S, Hata M, Fukumoto K, Yamane Y, Matsui T, Tamura A, Yonemura S, et al. (2002) Radixin deficiency causes conjugated hyperbilirubinemia with loss of Mrp2 from bile canalicular membranes. *Nat Genet* 31:320–325
- Kitajiri S, Fukumoto K, Hata M, Sasaki H, Katsuno T, Nakagawa T, Ito J, et al. (2004) Radixin deficiency causes deafness associated with progressive degeneration of cochlear stereocilia. *J Cell Biol* 166:559–570
- Kluin PM, Kramer MF, de Rooij DG (1984) Proliferation of spermatogonia and Sertoli cells in maturing mice. *Anat Embryol (Berl)* 169:73–78
- Kramer JM, Erickson RP (1981) Developmental program of PGK-1 and PGK-2 isozymes in spermatogenic cells of the mouse: specific activities and rates of synthesis. *Dev Biol* 87:37–45
- Lankes WT, Furthmayr H (1991) Moesin: a member of the protein 4.1-talin-ezrin family of proteins. *Proc Natl Acad Sci USA* 88:8297–8301
- Lee NP, Mruk DD, Conway AM, Cheng CY (2004) Zyxin, axin, and Wiskott-Aldrich syndrome protein are adaptors that link the cadherin/catenin protein complex to the cytoskeleton at adherens junctions in the seminiferous epithelium of the rat testis. *J Androl* 25:200–215
- Levine N, Marsh DJ (1971) Micropuncture studies of the electrochemical aspects of fluid and electrolyte transport in individual seminiferous tubules, the epididymis and the vas deferens in rats. *J Physiol* 213:557–570
- Lewis MJ, Lewis EH III, Amos JA, Tsongalis GJ (2003) Cystic fibrosis. *Am J Clin Pathol* 120(suppl):3–13
- Mangeat P, Roy C, Martin M (1999) ERM proteins in cell adhesion and membrane dynamics. *Trends Cell Biol* 9:187–192
- Mirza M, Hreinsson J, Strand ML, Hovatta O, Söder O, Philipson L, Pettersson RF, et al. (2006) Coxsackievirus and adenovirus receptor (CAR) is expressed in male germ cells and forms a complex with the differentiation factor JAM-C in mouse testis. *Exp Cell Res* 312:817–830
- Mueller S, Rosenquist TA, Takai Y, Bronson RA, Wimmer E (2003) Loss of nectin-2 at Sertoli-spermatid junctions leads to male infertility and correlates with severe spermatozoan head and midpiece

- malformation, impaired binding to the zona pellucida, and oocyte penetration. *Biol Reprod* 69:1330–1340
- Parlato S, Giammarioli AM, Logozzi M, Lozupone F, Matarrese P, Luciani F, Falchi M, et al. (2000) CD95 (APO-1/Fas) linkage to the actin cytoskeleton through ezrin in human T lymphocytes: a novel regulatory mechanism of the CD95 apoptotic pathway. *EMBO J* 19:5123–5134
- Pataky F, Pironkova R, Hudspeth AJ (2004) Radixin is a constituent of stereocilia in hair cells. *Proc Natl Acad Sci USA* 101:2601–2606
- Pawson T, Scott JD (1997) Signaling through scaffold, anchoring, and adaptor proteins. *Science* 278:2075–2080
- Russell LD, Ettlin RA, Sinha Hikim AP, Clegg ED (1990) *Histological and Histopathological Evaluation of the Testis*. Clearwater, FL, Cache River Press
- Saotome I, Curto M, McClatchey AI (2004) Ezrin is essential for epithelial organization and villus morphogenesis in the developing intestine. *Dev Cell* 6:855–864
- Serrador JM, Vicente-Manzanares M, Calvo J, Barreiro O, Montoya MC, Schwartz-Albiez R, Furthmayr H, et al. (2002) A novel serine-rich motif in the intercellular adhesion molecule 3 is critical for its ezrin/radixin/moesin-directed subcellular targeting. *J Biol Chem* 277:10400–10409
- Shestakova E, Vandekerckhove J, De Mey JR (1998) Epithelial and fibroblastoid cells contain numerous cell-type specific putative microtubule-regulating proteins, among which are ezrin and fodrin. *Eur J Cell Biol* 75:309–320
- Short DB, Trotter KW, Rezek D, Kreda SM, Bretscher A, Boucher RC, Stutts MJ, et al. (1998) An apical PDZ protein anchors the cystic fibrosis transmembrane conductance regulator to the cytoskeleton. *J Biol Chem* 273:19797–19801
- Siu MK, Cheng CY (2004) Interactions of proteases, protease inhibitors, and the beta1 integrin/laminin gamma3 protein complex in the regulation of ectoplasmic specialization dynamics in the rat testis. *Biol Reprod* 70:945–964
- Smith ME, Thomas JA (1990) Cellular expression of lymphocyte function associated antigens and the intercellular adhesion molecule-1 in normal tissue. *J Clin Pathol* 43:893–900
- Suzuki-Toyota F, Ishibashi K, Yuasa S (1999) Immunohistochemical localization of a water channel, aquaporin 7 (AQP7), in the rat testis. *Cell Tissue Res* 295:279–285
- Tamura A, Kikuchi S, Hata M, Katsuno T, Matsui T, Hayashi H, Suzuki Y, et al. (2005) Achlorhydria by ezrin knockdown: defects in the formation/expansion of apical canaliculi in gastric parietal cells. *J Cell Biol* 169:21–28
- Tsukioka F, Wakayama T, Tsukatani T, Miwa T, Furukawa M, Iseki S (2007) Expression and localization of the cell adhesion molecule SgIGSF during regeneration of the olfactory epithelium in mice. *Acta Histochem Cytochem* 40:43–52
- Tsukita S, Hieda Y, Tsukita S (1989) A new 82-kD barbed end-capping protein (radixin) localized in the cell-to-cell adherens junction: purification and characterization. *J Cell Biol* 108:2369–2382
- Tsukita S, Yonemura S (1999) Cortical actin organization: lessons from ERM (ezrin/radixin/moesin) proteins. *J Biol Chem* 274:34507–34510
- Turunen O, Wahlström T, Vaheri A (1994) Ezrin has a COOH-terminal actin-binding site that is conserved in the ezrin protein family. *J Cell Biol* 126:1445–1453
- Vaheri A, Carpén O, Heiska L, Helander TS, Jääskeläinen J, Majander-Nordenswan P, Sainio M, et al. (1997) The ezrin protein family: membrane-cytoskeleton interactions and disease associations. *Curr Opin Cell Biol* 9:659–666
- Vogl AW, Pfeiffer DC, Redenbach DM, Grove BD (1993) Sertoli cell cytoskeleton. In Russell LD, Griswold MD, eds. *The Sertoli Cell*. Clearwater, FL, Cache River Press, 39–86
- Wakayama T, Hamada K, Yamamoto M, Suda T, Iseki S (2003a) The expression of platelet endothelial cell adhesion molecule-1 in mouse primordial germ cells during their migration and early gonadal formation. *Histochem Cell Biol* 119:355–362
- Wakayama T, Kato Y, Utsumi R, Tsuji A, Iseki S (2006) A time- and cost-saving method of producing rat polyclonal antibodies. *Acta Histochem Cytochem* 39:79–87
- Wakayama T, Koami H, Ariga H, Kobayashi D, Sai Y, Tsuji A, Yamamoto M, et al. (2003b) Expression and functional characterization of the adhesion molecule spermatogenic immunoglobulin superfamily in the mouse testis. *Biol Reprod* 68:1755–1763
- Wakayama T, Sai Y, Ito A, Kato Y, Kurobo M, Murakami Y, Nakashima E, et al. (2007) Heterophilic binding of the adhesion molecules poliovirus receptor and immunoglobulin superfamily 4A in the interaction between mouse spermatogenic and Sertoli cells. *Biol Reprod* 76:1081–1090
- Wong CH, Cheng CY (2005) The blood-testis barrier: its biology, regulation, and physiological role in spermatogenesis. *Curr Top Dev Biol* 71:263–296
- Woodward AM, Crouch DH (2001) Cellular distributions of the ERM proteins in MDCK epithelial cells: regulation by growth and cytoskeletal integrity. *Cell Biol Int* 25:205–213
- Yonemura S, Hirao M, Doi Y, Takahashi N, Kondo T, Tsukita S, Tsukita S (1998) Ezrin/radixin/moesin (ERM) proteins bind to a positively charged amino acid cluster in the juxta-membrane cytoplasmic domain of CD44, CD43, and ICAM-2. *J Cell Biol* 140:885–895
- Yun CH, Lamprecht G, Forster DV, Sidor A (1998) NHE3 kinase A regulatory protein E3KARP binds the epithelial brush border Na⁺/H⁺ exchanger NHE3 and the cytoskeletal protein ezrin. *J Biol Chem* 273:25856–25863